

# Supporting Information

*for*

## Control of Metal-Organic Framework Crystal Topology by Ligand Functionalization: Functionalized HKUST-1 Derivatives

*Yang Cai, Ambarish Kulkarni, You-Gui Huang, David S. Sholl, and Krista. S. Walton\**

School of Chemical and Biomolecular Engineering, Georgia Institute of Technology, 311

Ferst Drive NW, Atlanta, Georgia 30332

## **Part 1: Experimental Details**

1. Synthesis procedure for ligands
  - 1.1 Preparation of methoxy-1,2,3-benzenetricarboxylic acid
  - 1.2 Preparation of bromo-1,2,3-benzenetricarboxylic acid
  - 1.3 Preparation of nitro-1,2,3-benzenetricarboxylic acid
  - 1.4 Preparation of acetamide-1,2,3-benzenetricarboxylic acid
2. Synthesis procedure for MOFs
  - 2.1 Preparation of fmj-methoxy
  - 2.2 Preparation of tbo-bromo
  - 2.3 Preparation of tbo-nitro
  - 2.4 Preparation of tbo-acetamide
3. Activation procedure for MOFs
  - 3.3 Activation of fmj-methoxy
  - 3.4 Activation of tbo-bromo
  - 3.5 Activation of tbo-nitro
  - 3.6 Activation of tbo-acetamide
4. Characterization
  - 4.1 SXRD (Single-crystal X-ray diffraction)
  - 4.2 PXRD (Powder X-ray Diffraction)
  - 4.3 NMR
  - 4.4 FT-IR
  - 4.5 Surface Area Analysis

## **Part 2: Computational Details**

## **EXPERIMENTAL DETAILS**

### **1. Synthesis procedure for ligands.**

All chemicals were obtained commercially and used without further purification. The ligands, methyl-1,3,5-benzenetricarboxylic acid and ethyl-1,3,5-benzenetricarboxylic acid were prepared as described in the literature <sup>1</sup>.

#### **1.1 Preparation of methoxy-1,3,5-benzenetricarboxylic acid (methoxy-BTC, Fig. S1)**

DMF was slowly added to a mixture of 2,6-bis(hydroxymethyl)-p-cresol (20g), K<sub>2</sub>CO<sub>3</sub> (32.73g) and CH<sub>3</sub>I (20.16g), with constant stirring (without heating) over a period of 3 days. A yellow milky solid was obtained, diluted with water, and then extracted with ethylacetate (EtOAc). The solvent was then removed in vacuo and the crude product was separated by a column separator (1:1 CH<sub>2</sub>Cl<sub>2</sub>: EtOAc) to yield 11.9g of **1**.

Sodium hydroxide (NaOH, 0.55g) was added to a mixture of **1** (5g) and water (165ml) in a 500 ml flask equipped with magnetic stirrer and oil bath. Potassium permanganate (KMnO<sub>4</sub>, 20.3g) was added in several batches to the solution over 2h while stirring and without heating. The solution was then heated at 80°C for 3 days with continuous stirring. The resultant brown slurry was filtered to remove the large amount of MnO<sub>2</sub>, and the filtrate was acidified with conc. HCl. The aqueous solution was continuously extracted with ethyl ether. Removal of the solvent (ethyl ether) in vacuo yields the product methoxy-BTC (3.6g). <sup>1</sup>H NMR (300 MHz, D<sub>2</sub>O): 8.33 (s, 2H), 3.73 (s, 3H).

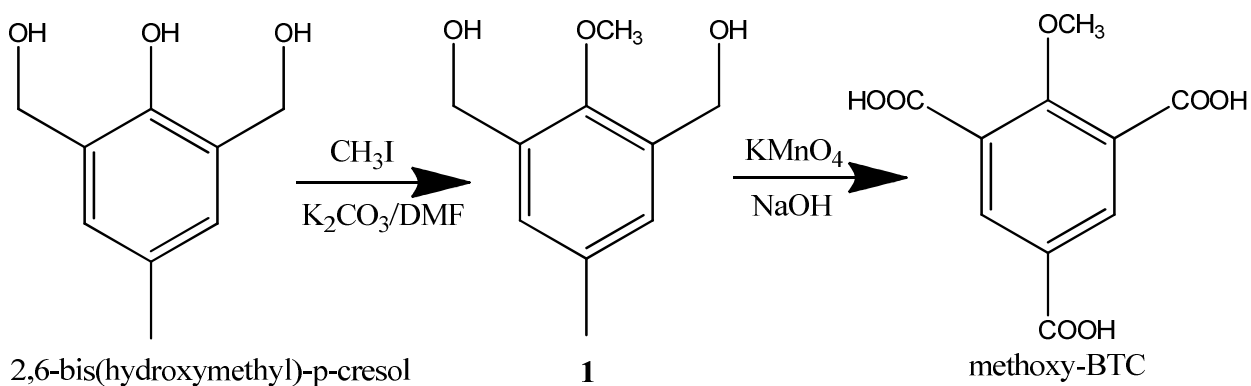


**Figure S1.** Synthesis procedure for methoxy-BTC

## 1.2 Preparation of bromo-1,3,5-benzenetricarboxylic acid (bromo-BTC, Fig. S2)

Initially, 2-bromomesitylene (20g) was added to an aqueous (250ml) solution of NaOH (5g). Potassium permanganate ( $\text{KMnO}_4$ , 85g) was added in several batches to the solution over a period of 2 h with stirring and without heating. Next, the solution was heated to  $95^\circ\text{C}$  with stirring for 3 days. The resultant brown slurry was then filtered to remove the large amount of  $\text{MnO}_2$ , and the filtrate was acidified with conc. HCl. The aqueous solution was continuously extracted with ethyl ether. Removal of the solvent (ethyl ether) in vacuo yields the product bromo-BTC (7.8g).  $^1\text{H}$  NMR (300 MHz, DMSO): 8.14 (s, 2H).

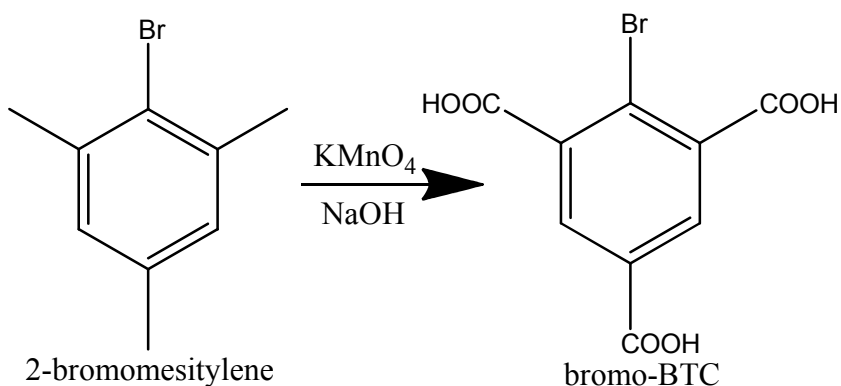


**Figure S2.** Synthesis procedure for bromo-BTC

### 1.3 Preparation of nitro-1,3,5-benzenetricarboxylic acid (nitro-BTC, Fig. S3)

2-nitromesitylene (20g) was added to an aqueous (250ml) solution of NaOH (5g). Potassium permanganate ( $\text{KMnO}_4$ , 85g) was added in several batches to the solution over 2 h with stirring and without heating, and the solution was heated to  $90^\circ\text{C}$  with stirring for 3 days. The resultant brown slurry was then filtered to remove the large amount of  $\text{MnO}_2$ , and the filtrate was acidified with conc. HCl. The aqueous solution was then continuously extracted with ethyl ether and removal of the solvent (ethyl ether) in vacuo affords product nitro-BTC (5g).  $^1\text{H}$  NMR (300 MHz, DMSO): 8.27 (s, 2H).

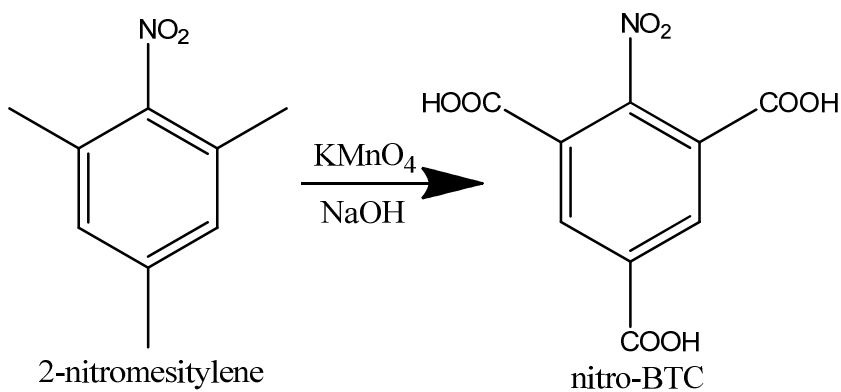


**Figure S3.** Synthesis procedure for nitro-BTC

### 1.4 Preparation of acetamide-1,3,5-benzenetricarboxylic acid (acetamide-BTC, Fig. S4)

A solution of 2,4,6-trimethyl-phenylamine (20g) in  $\text{CH}_2\text{Cl}_2$  (200ml) was cooled to  $0^\circ\text{C}$  (ice-water bath). To this, acetyl chloride ( $\text{AcCl}$ , 11.92g) was gradually added over a period 5 minutes via an addition funnel and this was followed by portion-wise addition of triethylamine ( $\text{Et}_3\text{N}$ , 15.4g). The ice-bath was removed and the solution was allowed to warm to room temperature and stirred for 2h. The resultant ivory colored solid was collected by filtration and dried in vacuo. To remove the residual  $\text{Et}_3\text{NHCl}$ , the solid was suspended in

water H<sub>2</sub>O (240ml) and stirred for 0.5 h, and collected by filtration and dried to a constant weight, which results 15g compound **2**.

Sodium hydroxide (NaOH, 0.55g) was added to a mixture of compound **2** (5g) and water (165ml), in a 500ml flask equipped with magnetic stirrer and oil bath,. Potassium permanganate (KMnO<sub>4</sub>, 34g) was added in several batches to the solution over 2h with stirring and without heating. Subsequently, the solution was heated to 85°C with stirring for 3days. The resultant brown slurry was then filtered to remove the large amount of MnO<sub>2</sub>, and the filtrate was acidified with conc. HCl. The aqueous solution is continuously extracted with ethyl ether. Removal of the solvent (ethyl ether) in vacuo yields product acetamide-BTC. <sup>1</sup>H NMR (300 MHz, D<sub>2</sub>O): 8.47 (s, 2H), 2.21 (s, 3H).

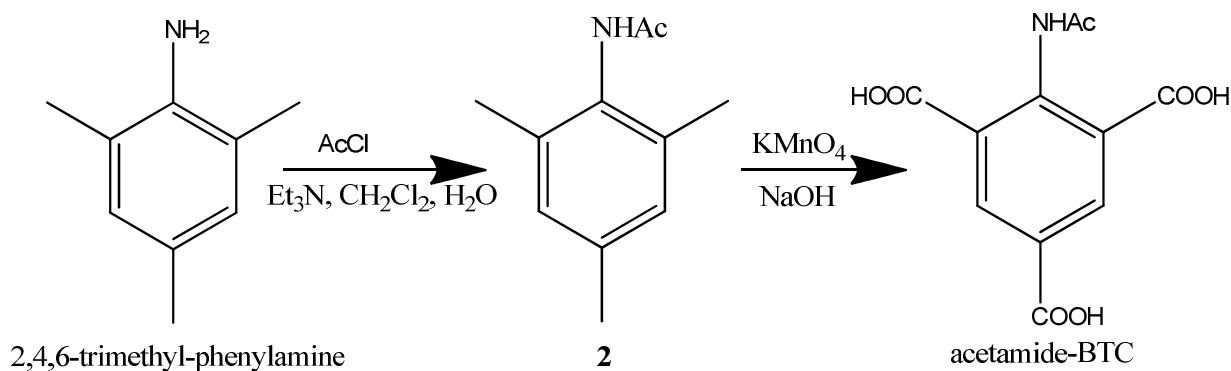


**Figure S4.** Synthesis procedure for acetamide-BTC

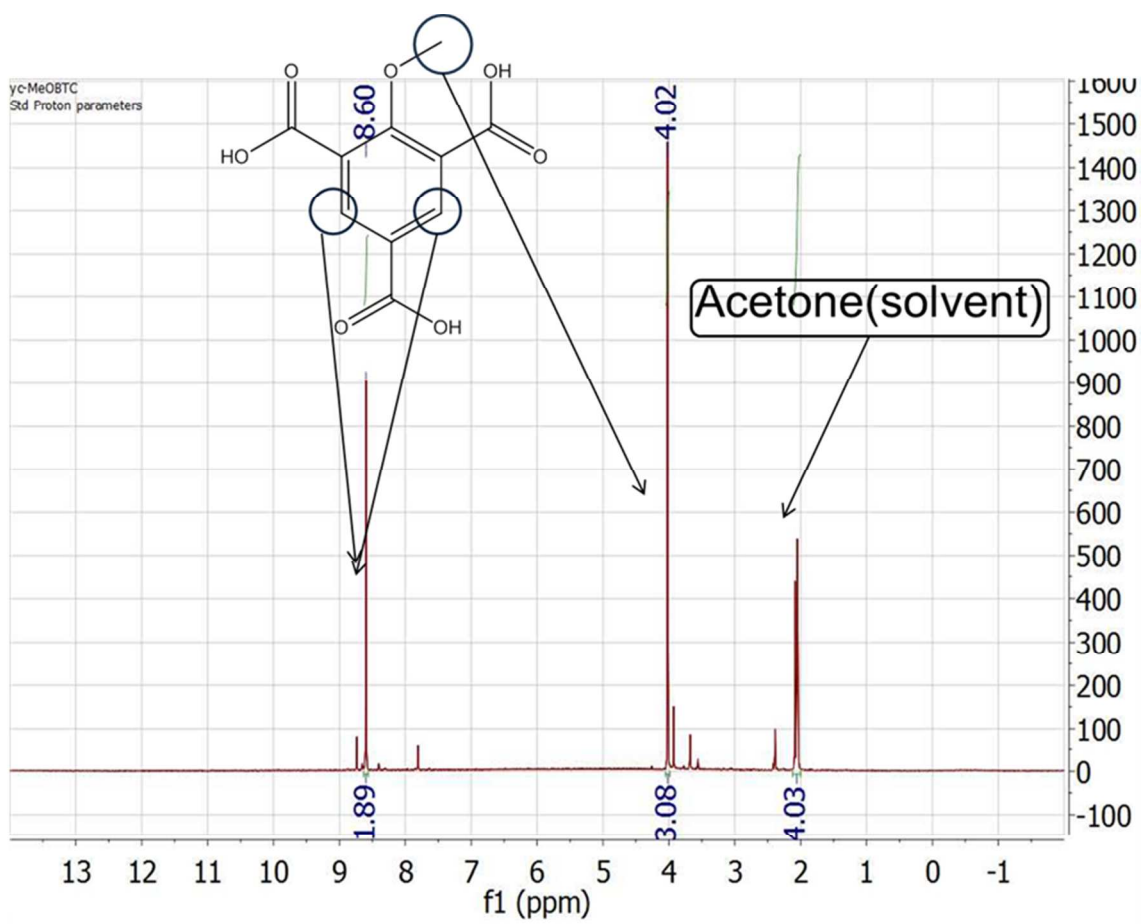


**Figure S5.** NMR of 2-methoxy-1,3,5-BTC.

## 2. Synthesis procedure for MOFs.

Experimental synthesis details for fmj-methyl and fmj-ethyl can be found in our previous work<sup>1</sup>. The synthesis procedure used for the other MOFs is described below. Solvents used for the synthesis are summarized in Table S1.

### 2.1 Synthesis of fmj-methoxy: single crystal (a) and powder material (b).

The single crystal form and powder form of fmj-methoxy were obtained using different synthesis conditions as described below.

- a. Single crystal form: A mixture of  $\text{Cu}(\text{NO}_3)_2 \cdot 3\text{H}_2\text{O}$  (72.48 mg), methoxy-BTC (48 mg), and DMF (6 ml) with 1M HCl aqueous solution (0.25 ml) was placed in a 20 ml glass vial and heated in a conventional oven at 80<sup>0</sup>C for 72 h. The block shaped green crystal is formed after cooling to room temperature.
- b. Powder form: A mixture of  $\text{Cu}(\text{NO}_3)_2 \cdot 3\text{H}_2\text{O}$  (72.48 mg), methoxy-BTC (48 mg), and DMF (6 ml) was placed in a 20 ml glass vial, and the resulting mixture was heated in a conventional oven at 70<sup>0</sup>C for 72 h and cooled to room temperature. The green powder material was obtained by filtration and washed with DMF. The yield was 65 mg.

### 2.2 Synthesis of tbo-bromo.

A mixture of  $\text{Cu}(\text{NO}_3)_2 \cdot 3\text{H}_2\text{O}$  (72.48 mg), bromo-BTC (58 mg), and DMF with 15 equivalents formic acid (with respect to  $\text{Cu}(\text{NO}_3)_2 \cdot 3\text{H}_2\text{O}$ ) was placed in a 20 ml glass vial. The mixture was heated in a conventional oven at 90<sup>0</sup>C for 48 h and cooled to room temperature. The green crystal was obtained by filtration and washed with DMF. The yield was 52mg.



### **2.3 Synthesis of tbo-nitro.**

A mixture of  $\text{Cu}(\text{NO}_3)_2 \cdot 3\text{H}_2\text{O}$  (72.48 mg), nitro-BTC (51 mg), and DMF with 1M HCl aqueous solution (0.15 ml) was placed in a 20 ml glass vial, and the resulting mixture was heated in a conventional oven at 120 °C for 60 h and cooled to room temperature. The green crystal was obtained by filtration and washed with DMF. The yield was 55mg.

### **2.4 Synthesis of tbo-acetamide.**

A mixture of  $\text{Cu}(\text{NO}_3)_2 \cdot 3\text{H}_2\text{O}$  (72.48 mg), acetamide-BTC (53.4 mg), and DMF with 1M HCl aqueous solution (0.15 ml) was placed in a 20 ml glass vial, and the resulting mixture was heated in a conventional oven at 100 °C for 72 h and cooled to room temperature. The green product was obtained by filtration and washed with DMF. The yield was 57mg.

### **3. Activation procedure for MOFs**

Activation procedure of fmj-methyl and fmj-ethyl can be found in our previous work <sup>1</sup>. The activation procedures used for the other MOFs are described below. The activation process has a significant impact on the adsorption capacity, surface areas. The activation procedures for all materials are summarized in the Table. S1

#### **3.1 Activation of fmj-methoxy**

The material was air-dried and was heated at 170°C under vacuum for 8h.

#### **3.2 Activation of tbo-bromo**

To remove the solvated DMF, the material was soaked in 20ml of methanol for 2 days, with the solvent decanted and refreshed daily. The material was air-dried and was heated at 170°C under vacuum for 8h.

#### **3.3 Activation of tbo-nitro**

To remove the solvated DMF, the material was soaked in 20ml of ethanol for 3 days, with the solvent decanted and refreshed daily. The material was air-dried and was heated at 170°C under vacuum for 8h.

#### **3.4 Activation of fmj-acetamide**

To remove the solvated DMF, the material was soaked in 20ml of methanol for 2 days, with the solvent decanted and refreshed daily. The material was air-dried and was heated at 170°C under vacuum for 8h.

**Table S1.** Summary of synthesis solvents, decomposition temperatures and activation procedures of all materials

MOFs	Synthesis Solvents	Decomposition temperatures (°C)	Activation procedure (under vacuum)
fmj-methyl	DMF	350 <sup>1</sup>	170°C, 8h
fmj-ethyl	Water/ EtOH	350 <sup>1</sup>	170°C, 8h
fmj-methoxy	DMF	300	170°C, 8h
tbo-bromo	DMF/ Formic acid	300	2d methanol exchange, 170°C, 8h
tbo-nitro	DMF/HCl sol.	280	3d ethanol exchange, 170°C, 8h
tbo-acetamide	DMF/HCl sol.	280	2d methanol exchange, 170°C, 8h

## 4. Characterization

### 4.1 SXRD (Single-crystal X-ray diffraction)

Single-crystal XRD data of fmj-methoxy was collected on a single crystal Bruker APEX CCD diffraction system with CuK $\alpha$  radiation. The structures were solved by direct methods, and refined by full-matrix least-squared techniques using SHELX-97.

**Table S2.** Crystallographic data for fmj-methoxy. <sup>a</sup>  $R = \sum ||F_0| - |F_c|| / \sum |F_0|$ , <sup>b</sup>  $wR = [\sum w(F_0 - F_c)^2 / \sum w(F_0^2)]^{1/2}$

Compound	fmj-methoxy
Formula	C <sub>20</sub> H <sub>14</sub> Cu <sub>3</sub> O <sub>15.75</sub>
Molecular weight (g mol <sup>-1</sup> )	689.93
Crystal size(mm)	0.22 × 0.20 × 0.12
Space group	Immm
<i>a</i> (Å)	19.4476(7)
<i>b</i> (Å)	19.448(5)
<i>c</i> (Å)	24.1299(8)
<i>V</i> (Å <sup>3</sup> )	9126.2(4)
<i>Z</i>	8
$\lambda(Cu\ K\alpha)$ (Å)	1.54178
<i>D</i> <sub>calcd</sub> (g cm <sup>-3</sup> )	1.014
$\mu$ (mm <sup>-1</sup> )	1.428
Temperature (K)	173(2)
Total reflections	23275
Unique data collected	4072
Observed reflections	2845
<i>R</i> <sub>int</sub>	0.1209
Parameters	195
<i>R</i> <sub>1</sub> , <i>wR</i> ( <i>I</i> > 2σ( <i>I</i> )) <sup>a</sup>	0.1138
<i>R</i> <sub>1</sub> , <i>wR</i> (all data) <sup>b</sup>	0.3525
<i>w</i> =1/ [σ <sup>2</sup> ( <i>F</i> <sub>o</sub> <sup>2</sup> )+( <i>aP</i> ) <sup>2</sup> + <i>bP</i> ]	<i>a</i> = 0.2000, <i>b</i> =0.0000
Goodness-of-fit-on <i>F</i> <sup>2</sup>	1.251
Δρ <sub>min</sub> and Δρ <sub>max</sub> (e Å <sup>-3</sup> )	-0.886, 1.826

As shown in Fig. S5, the fmj-methoxy has the same topology as fmj-methyl and fmj-ethyl<sup>1</sup>.

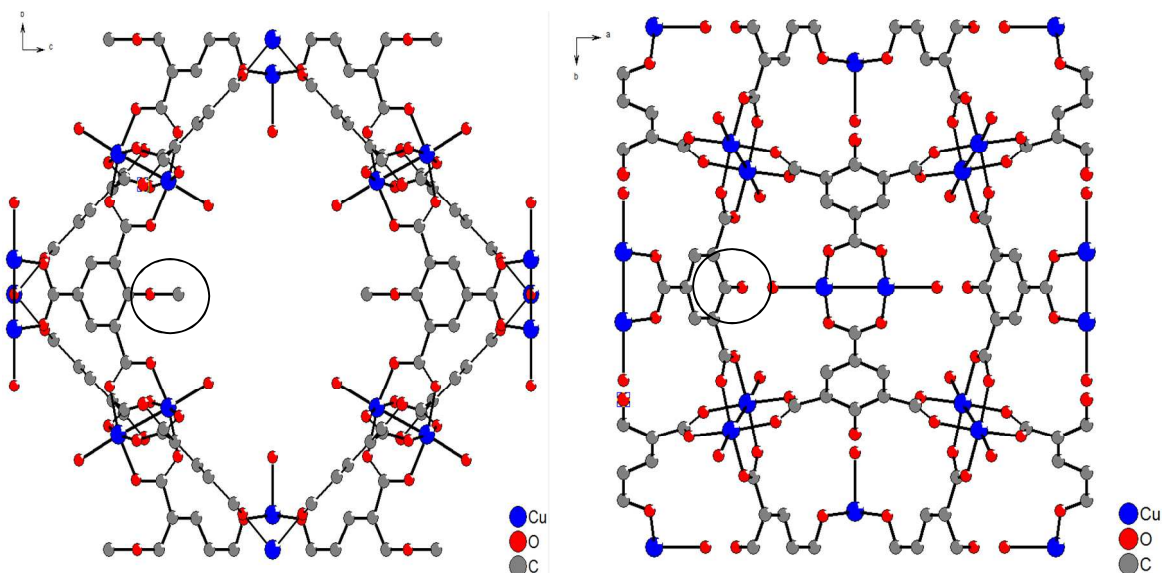


**Figure S6.** Frameworks of fmj-methoxy viewed along the [100] (a) and [010] (b) direction

#### 4.2 PXRD (Powder X-ray diffraction)

Despite numerous synthesis attempts, we were unable to obtain single crystals of functionalized tbo series MOFs suitable for single-crystal XRD measurements. Thus, powder XRD (Fig. S6) was used to confirm that the nitro, acetamide and bromo functionalized product was isostructural with the tbo topology of parent HKUST-1. As showed in Fig. S6, the PXRD patterns of tbo-bromo, tbo-nitro, and tbo-acetamide are consistent with the HKUST-1 patterns <sup>2</sup>.

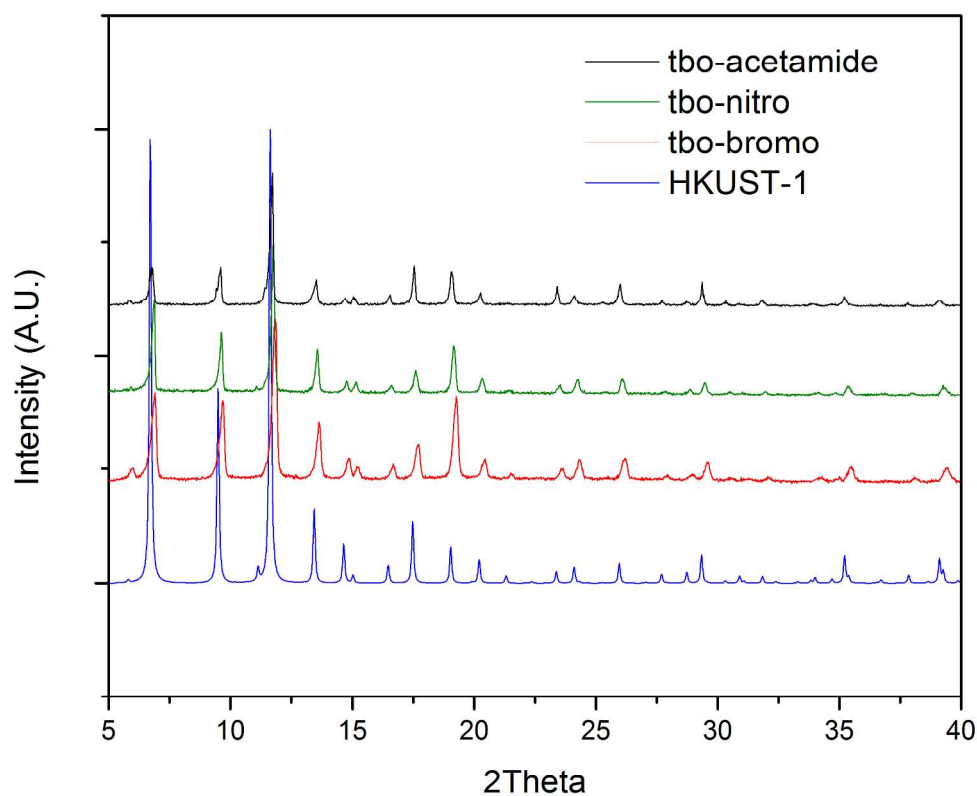


**Figure S7.** Powder X-ray diffractograms of nitro, acetamide, bromo functionalized MOF in the tbo topology and comparison with parent HKUST-1<sup>2</sup>

The simulated PXRD of the fmj-methyl<sup>1</sup>, fmj-ethyl<sup>1</sup>, and fmj-methoxy materials was obtained from single-crystal x-ray diffraction studies on single crystal. Fig. S7 shows that as-synthesized materials of fmj-methoxy, fmj-methyl and fmj-ethyl have the same structure with single crystal. The slight shifting of the peaks may arise from differences in the lattice constants.

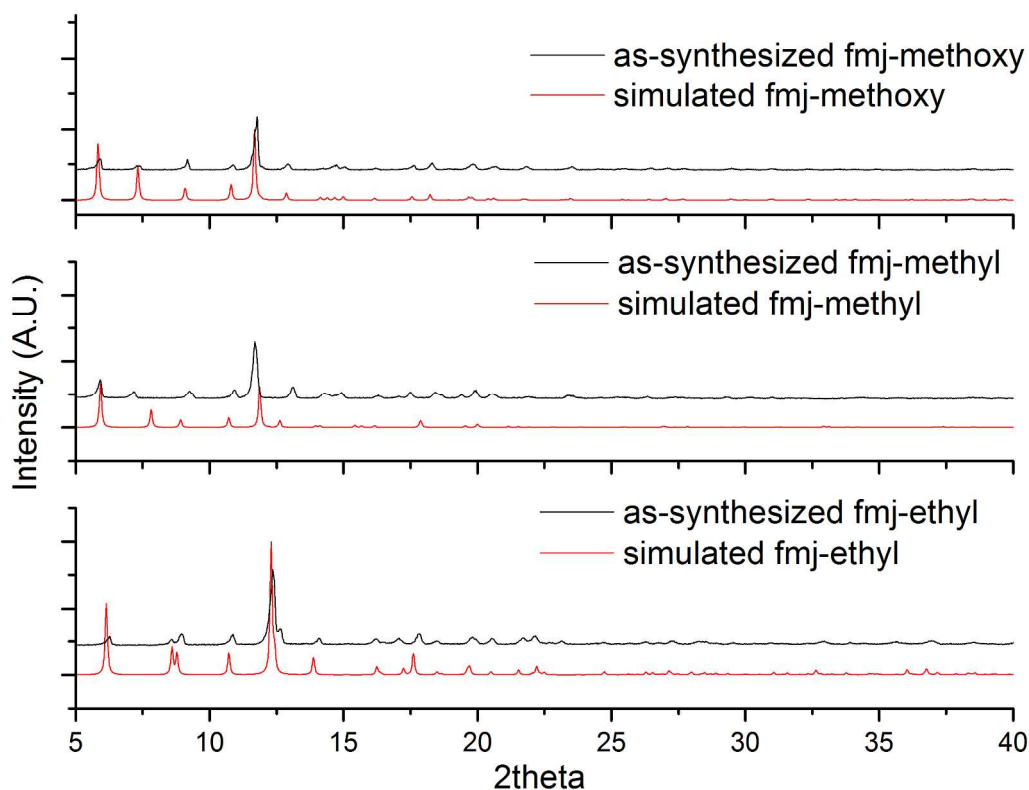
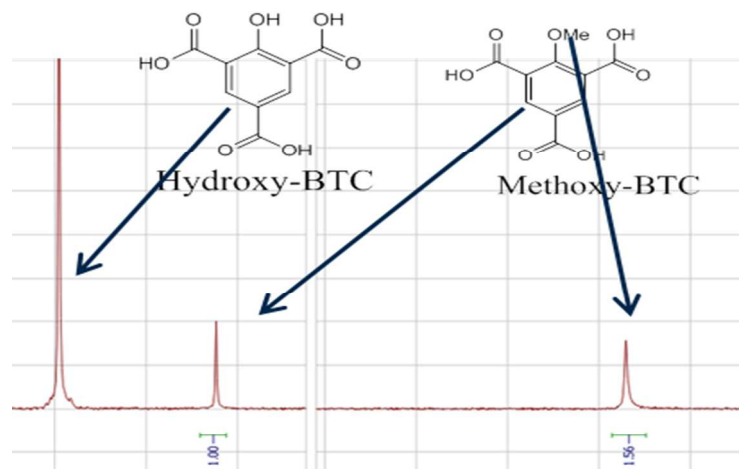


**Figure S8.** Comparison of PXRD pattern for as-synthesized fmj-methoxy, fmj-methyl, and fmj-ethyl and simulated pattern from single crystal data

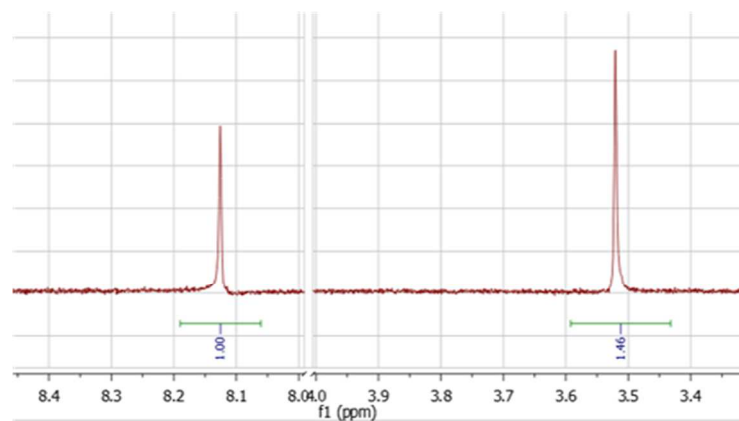
### 4.3 Nuclear Magnetic Resonance (NMR)

Single crystal of fmj-methoxy is synthesized under different condition with powder-form materials of fmj-methoxy. Based on the PXRD pattern comparison in Fig. S7 showed that the powder materials of fmj-methoxy has the same structure with single crystal. NMR studies were used to verify the presence of methoxy functional group.

As shown in Fig. S8, there are only methoxy functional groups in powder materials of fmj-methoxy, while the methoxy functional groups in single crystal materials were partially decomposed to hydroxyl groups.



(a)



(b)

**Figure S9.** NMR data of single crystal (a) of fmj-methoxy and powder material (b) of fmj-methoxy



#### 4.4 FT-IR

The presence of the functional groups (nitro, bromo, and acetamide) on the linkers was further investigated by means of FTIR spectroscopy. Before acquiring the spectra, the samples were activated under vacuum to remove the residual solvent and then prepared as a KBr pellet. From Fig. S9, the typical absorption modes of the nitro, bromo, and acetamide groups are clearly visible in the functionalized MOFs, which confirms the effective functionalization of the internal pore surface. The IR spectra of the unfunctionalized parent HKUST-1 is also shown for comparison.

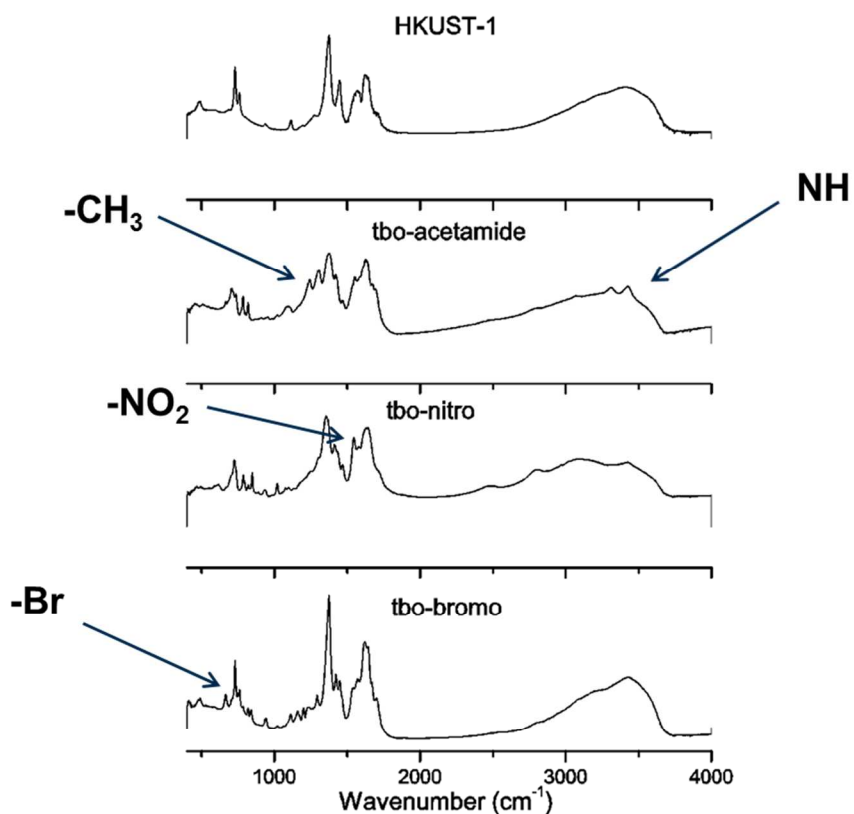


**Figure S10.** FTIR spectra of tbo-X (X=H, nitro, bromo, acetamide) activated at 120<sup>0</sup>C in vacuum.

## 4.5 TGA

Thermal stability of the various MOFs was measured using TGA experiments, showed in Fig. S10. The decomposition temperatures of fmj-methoxy (300 °C), tbo-bromo (300 °C), tbc-nitro (280 °C), and tbc-acetamide (280 °C) were found to be slightly lower than the methyl or ethyl functionalized MOFs (350 °C) reported earlier<sup>1</sup>. The decomposition temperatures for all materials are summarized in Table S1.

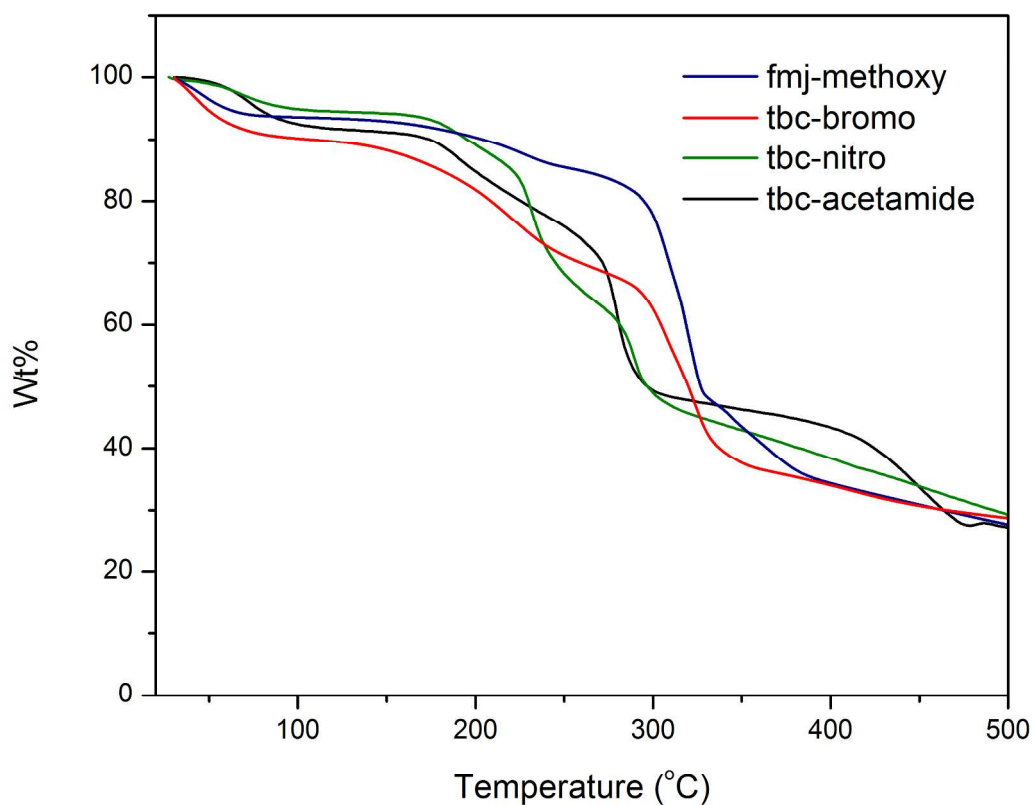


**Figure S11.** TGA curve of as-synthesized fmj-methoxy, tbo-bromo, tbo-nitro, and tbo-acetamide in nitrogen flux

#### 4.6 Surface area analysis

The theoretical accessible surface area<sup>3</sup> is calculated by rolling a spherical probe along the surface of MOFs. All values are reported for a N<sub>2</sub> probe diameter of 3.681 Å. Nitrogen adsorption isotherms of fmj-methoxy, tbo-bromo, tbo-nitro, tbo-acetamide at 77 K are reported in Fig. S11 - S14, and are used to obtain the BET surface areas of the activated MOFs. The measured surface areas and the accessible surface areas are summarized in Table 1 of the main text.

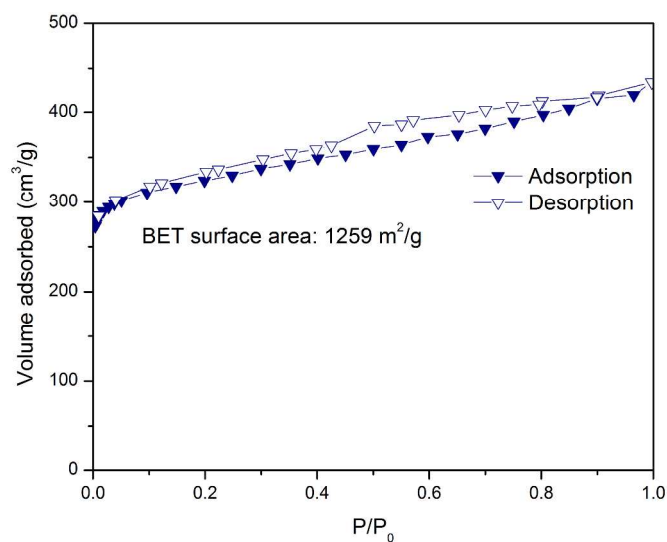


**Figure S12.** Nitrogen isotherm of activated fmj-methoxy at 77K (closed symbols – adsorption, open symbols – desorption)

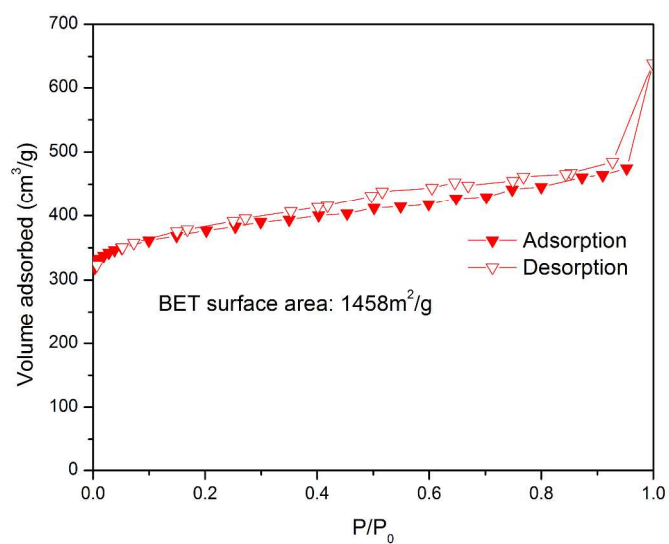


**Figure S13.** Nitrogen isotherm of activated tbo-bromo at 77K (closed symbols – adsorption, open symbols – desorption)

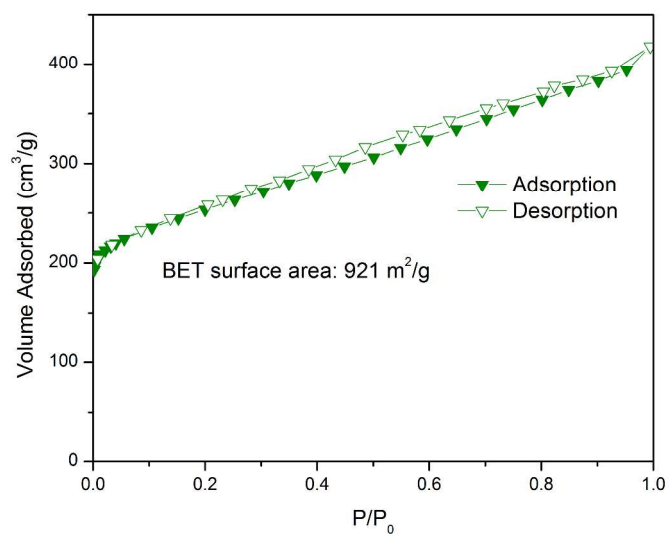


**Figure S14.** Nitrogen isotherm of activated tbo-nitro at 77K (closed symbols – adsorption, open symbols – desorption)

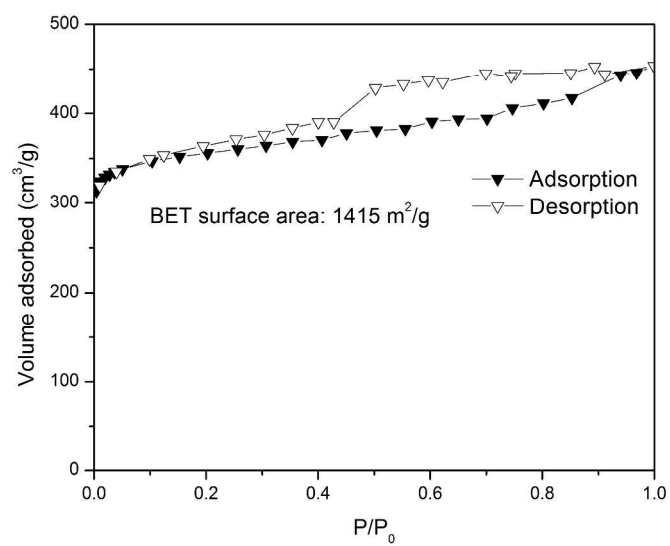


**Figure S15:** Nitrogen isotherm of activated tbo-acetamide at 77K (closed symbols – adsorption, open symbols – desorption)

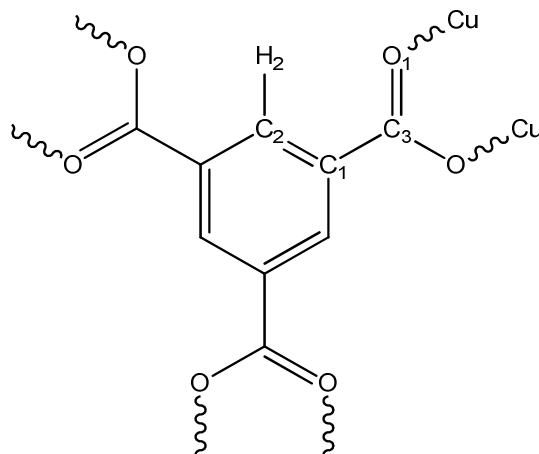
## COMPUTATIONAL DETAILS

**Table S3.** Comparison of average bond lengths and angles from DFT-D2 optimization to the experimental structure of HKUST-1<sup>2</sup>

Bond length (Å)	Expt.	DFT-D2
C1-C3	1.5	1.5
C1-C2	1.4	1.4
C2-H2	1.1	0.9
C3-O1	1.3	1.3
O1-Cu	2.0	2.0
Cu-Cu	2.5	2.6

Angle (Deg.)	Expt.	DFT-D2
C1-C2-C1	119.9	120.1
C2-C1-C2	120.1	119.8
C3-C1-C2	119.9	120.0
C3-O1-Cu	119.6	123.1
H2-C2-C1	120.0	119.9
O1-C3-O1	126.3	125.6
C1-C3-O1	116.8	117.2
O1-Cu-Cu	87.2	84.1

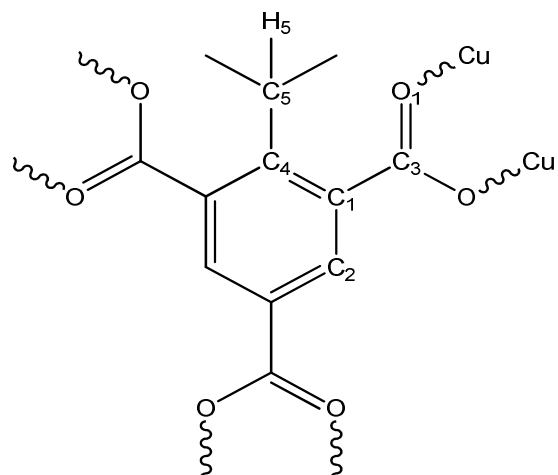


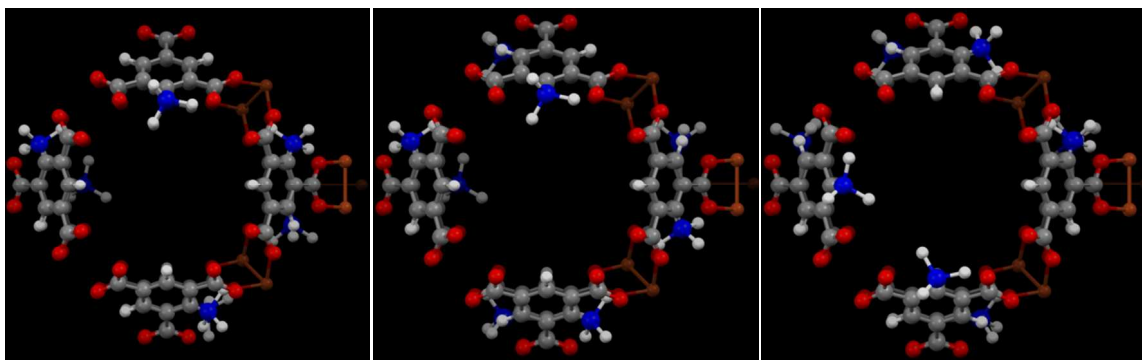
**Table S4.** Comparison of average bond lengths and angles from DFT-D2 optimization to the experimental structure of fmj-methyl from <sup>1</sup>

Bond length (Å)	Expt.	DFT-D2
C1-C3	1.5	1.5
C1-C2	1.4	1.4
C2-H2	1.0	1.1
C3-O1	1.2	1.3
O1-Cu	1.9	2.0
Cu-Cu	2.6	2.5
C4-C1	1.4	1.4
C4-C5	1.5	1.5

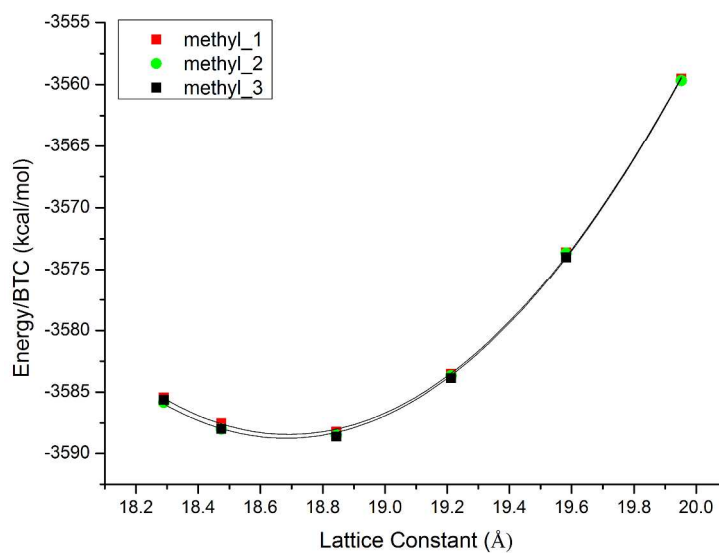
  

Angle (Deg.)	Expt.	DFT-D2
C1-C2-C1	116.3	120.3
C2-C1-C2	126.7	119.2
C3-C1-C2	114.2	117.6
C3-O1-Cu	125.6	119.4
H2-C2-C1	121.8	119.9
O1-C3-O1	122.1	126.9
C1-C3-O1	118.9	116.5
O1-Cu-Cu	83.0	87.0
O1-Cu-O1	89.1	89.8
C1-C4-C1	122.0	116.1
C2-C1-C4	118.8	122.0
C3-C1-C4	128.8	123.2





**Figure S16.** Three examples of choosing random positions for replacement of H atom by the methyl group for every BTC linker. Carbon atom of the replaced methyl group is shown in blue.



**Figure S17.** Results of DFT-D2 energy minimization for the three instances of methyl functionalized BTC linkers in the tbo topology (shown in (a)). The energies are obtained at different values of the lattice constants for each case. The minimum obtained after fitting a parabolic curve (black solid line) is used as the energy of the material.



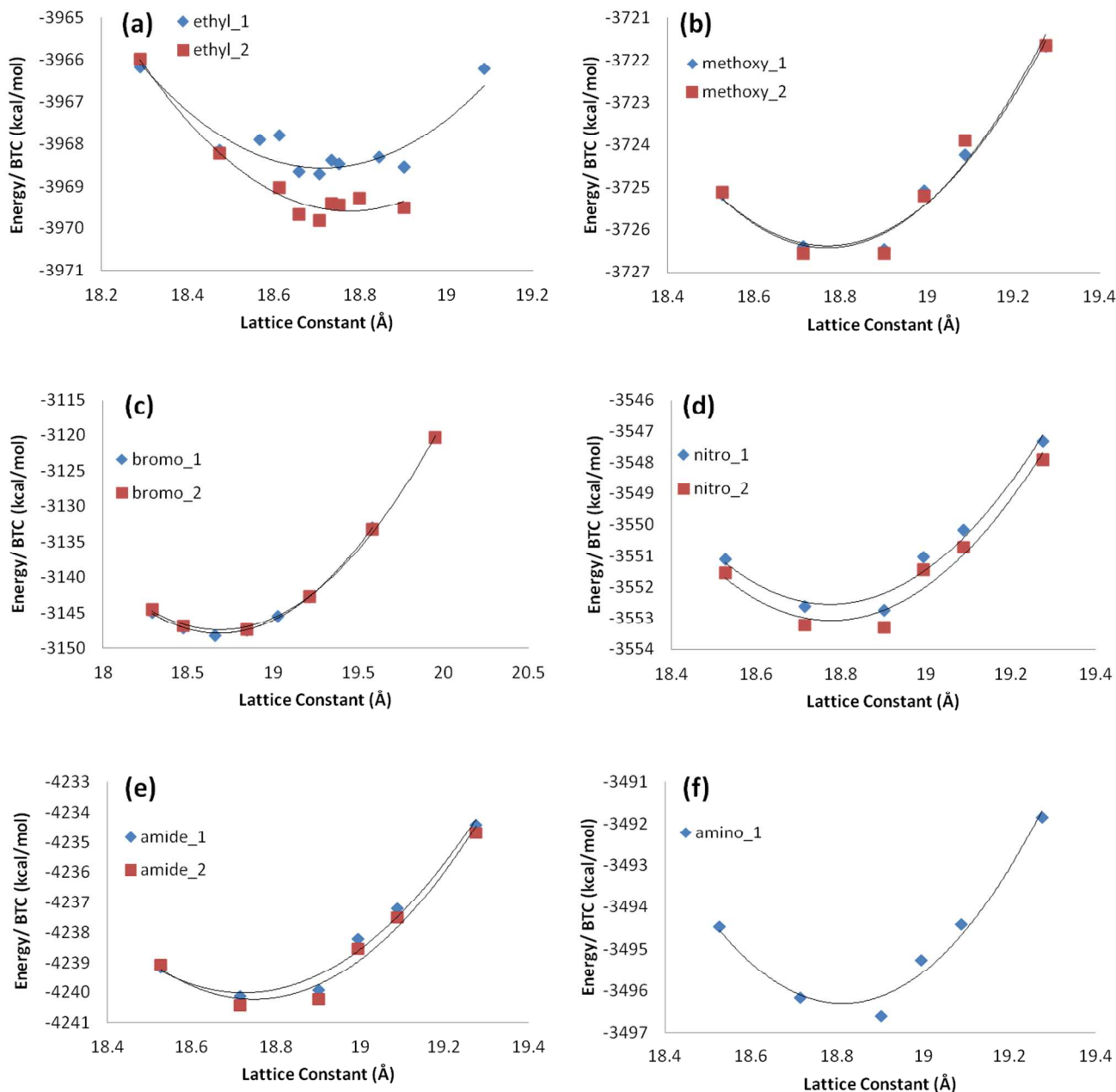


**Figure S18.** DFT-D2 energy minimization for the multiple instances of functionalized BTC linkers in the tbo topology for (a) ethyl, (b) methoxy, (c) bromo, (d) nitro, (e) acetamide and (f) amino functionalized BTC. The energies are obtained at different values of the lattice constants for each case. The minimum obtained after fitting a parabolic curve (black solid line) is used as the energy of the material.

**Table S5.** Fitting parameters for the parabolic function used to obtain the minimum energy of a material in the tbo topology. The parabolic function is defined as  $E = a_{fit}x^2 + b_{fit}x + c_{fit}$ , where E is the energy and x is the lattice constant of the periodic structure.  $x_{optim}$  refers to the lattice constant corresponding to the minimum energy.

	$a_{fit}$	$b_{fit}$	$c_{fit}$	DFT-D2 (kcal/mol-linker)	DFT (kcal/mol-linker)	vdW (kcal/mol-linker)	$x_{optim}$ *
<b>H-BTC</b>	-	-	-	-3210.1	-3189.1	-21.0	18.7
<b>methyl</b>	18.2	-678.3	2746.8	-3588.8	-3563.5	-25.3	18.7
<b>ethyl</b>	15.3	-574.2	1420.4	-3969.6	-3940.2	-29.4	18.8
<b>methoxy</b>	19.6	-737.5	3194.9	-3726.4	-3699.5	-27.0	18.8
<b>bromo</b>	18.4	-687.7	3275.9	-3147.9	-3124.2	-23.7	18.7
<b>nitro</b>	21.6	-812.5	4074.7	-3553.1	-3528.4	-24.7	18.8
<b>acetamide</b>	20.7	-776.2	3035.3	-4240.2	-4208.4	-31.8	18.7
<b>amino</b>	21.6	-813.7	4157.3	-3496.3	-3472.7	-23.6	18.8

**Table S6.** The minimum DFT-D2 energy corresponding to each functionalized linker for the tbo, pto and fmj topology. The underlined values represent the minimum of the three topologies. In all the cases the pto topology is found to be more unfavorable than the fmj and/or the tbo topology.

Functional group	DFT-D2 (kcal/mol-linker)		
	tbo	pto	fmj
<b>H-BTC</b>	<u>-3210.1</u>	-3207.3	-3206.8
<b>methyl</b>	-3588.5	-3589.5	<u>-3590.1</u>
<b>ethyl</b>	-3969.8	-3973.0	<u>-3973.6</u>
<b>methoxy</b>	-3726.6	-3723.1	<u>-3727.4</u>
<b>bromo</b>	-3148.2	-3150.4	<u>-3151.7</u>
<b>nitro</b>	<u>-3553.3</u>	-3553.2	-3550.3
<b>acetamide</b>	<u>-4240.4</u>	-4226.5	-4236.5
<b>amino</b>	<u>-3496.3</u>	-3495.8	-3495.5

**Table S7.** Structural parameters of the minimum energy configurations for the various functionalized clusters obtained from the contour plots.

<b>Linker</b>	<b>Structural Parameters (<math>\theta, \phi</math>)</b>
<b>H-BTC</b>	120°, 0°
<b>methyl</b>	124°, 40°
<b>ethyl</b>	124°, 50°
<b>methoxy</b>	123°, 50°
<b>bromo</b>	123°, 60°
<b>nitro</b>	123°, 0°
<b>amino</b>	125°, 0°

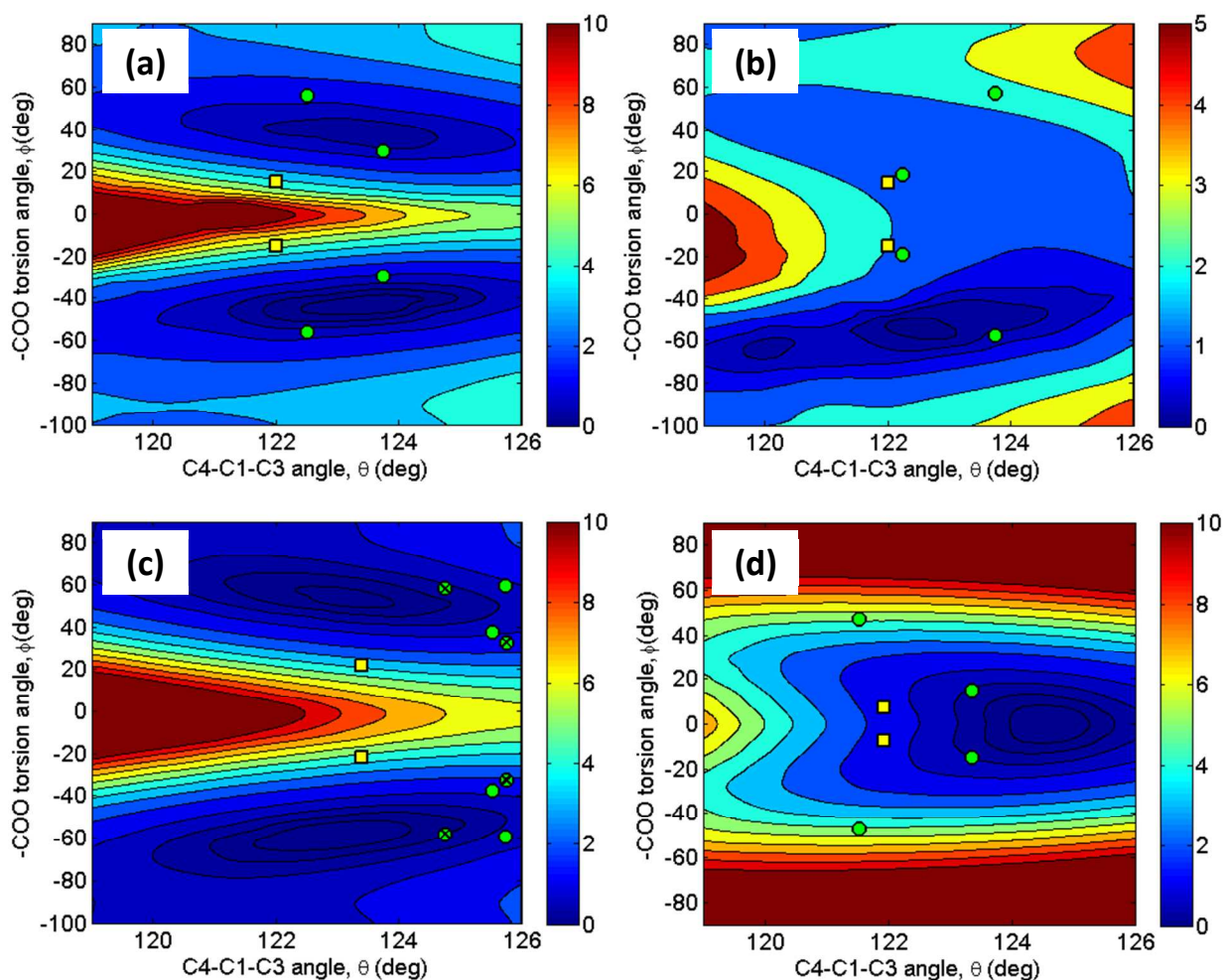


**Fig. S19** Contour plots of energy as a function of  $\phi$  and  $\theta$  for (a) methyl, (b) methoxy (c) bromo and (d) amino-BTC linkers. The yellow squares and green circles represent the structural parameters from the DFT-D2 optimized tbo and fmj topology respectively. For bromo-BTC (c), the green circles and the crossed green circles represents the structural parameters for two energy minimized fmj structures, each having different lattice parameters.

## Electron Localization Function (ELF) analysis for methyl, nitro and methoxy-BTC

The electron localization function (ELF) calculations were performed using VASP and the surfaces at an iso-value of 0.87 was used to generate the images. Only the electron density around the functional group is shown for clarity.

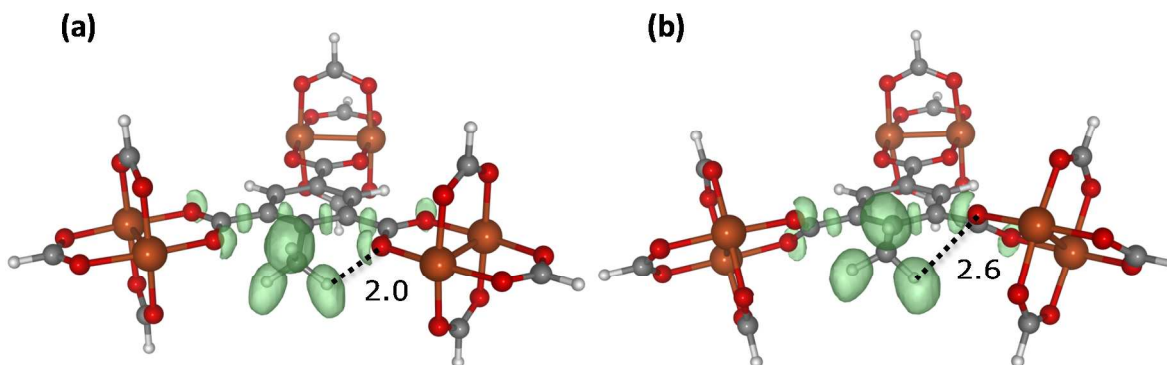


**Figure S20.** ELF for methyl-BTC for (a) the ideal tbo configuration and (b) the minimum energy configuration

ELF for  $\theta = 120^\circ$  and  $\phi = 0^\circ$  for the methyl-BTC cluster is shown in Fig. 7 (a) of the main text. The C atom of the methyl group is  $sp^3$  hybridized and is not planar with the benzene ring. This is due to the interaction of the oxygen lone pairs of the ortho carboxylate groups ( $O_{ortho}$ ) with the H atoms of the methyl group and the distance is  $\sim 2 \text{ \AA}$ . From the contour plot calculations, the minimum energy of the cluster corresponds to  $\theta = 124^\circ$  and  $\phi = 40^\circ$  and the ELF is shown in Fig. 7 (b). Both the carboxylate groups are twisted out of the plane so as to decrease the steric hindrance of the functional group with the carboxylate entity. The H-  $O_{ortho}$  distance now increases by  $> 25\%$  to  $2.6 \text{ \AA}$ . We conclude for the methyl group, it is the C-H bond of the connecting  $sp^3$  C atom that leads to the torsion of the carboxylate groups.

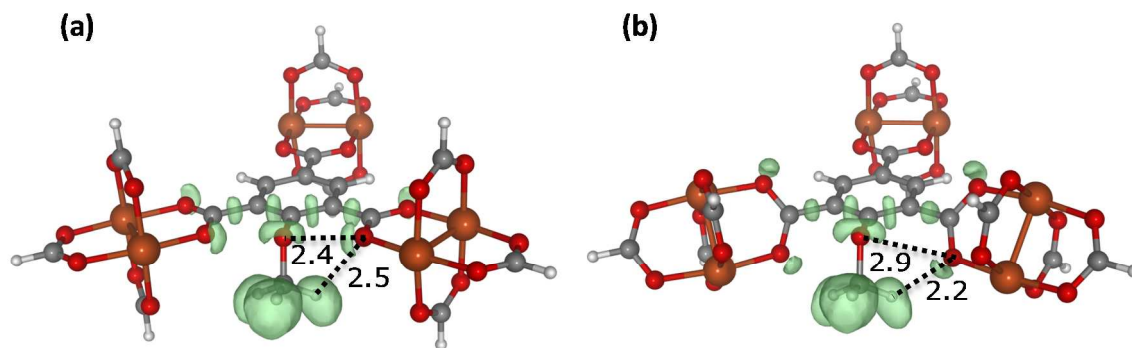


**Figure S21.** ELF for methoxy-BTC for (a) the ideal tbo configuration and (b) the minimum energy configuration

The oxygen atom of the methoxy group is  $sp^3$  hybridized; two of the 3  $sp^3$  orbitals are occupied by lone pairs of electrons. Fig. S20 (a) and (b) shows the ELF for the ideal tbo cluster configuration and the minimum energy configuration for the methoxy-BTC linker. Here, the torsion of the carboxylate group is such that the lone pair on carboxylate oxygen atoms points away from the lone pairs on the oxygen atom of the methoxy functional group and increases the  $O_{\text{methoxy}}-O_{\text{ortho}}$  from 2.4 to 2.9 Å. Also, this torsion of the carboxylate group decreases the  $H_{\text{methoxy}}-O_{\text{ortho}}$  distance from 2.4 Å to 2.2 Å showing that the lone pair repulsion is a stronger effect than the C-H bond of the methyl group.

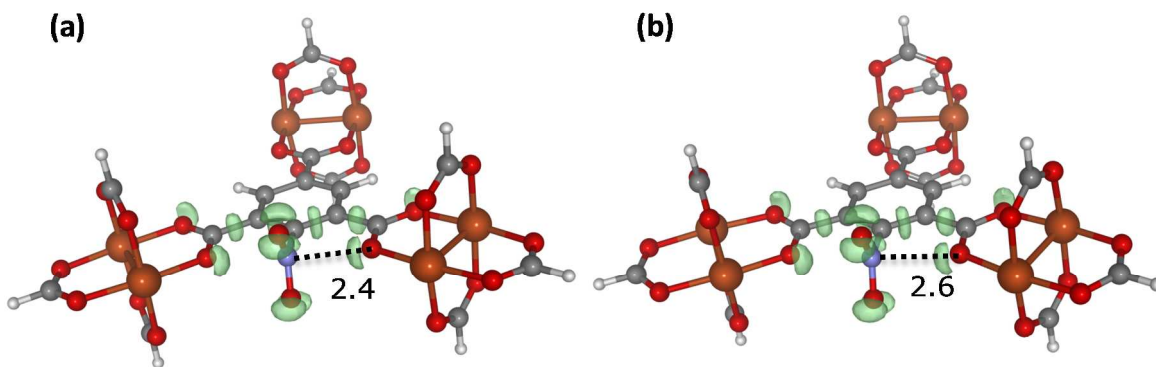


**Figure S22.** ELF for nitro-BTC for (a) the ideal tbo configuration and (b) the minimum energy configuration

The ELF for the ideal configuration ( $\theta = 120^\circ$  and  $\phi = 0^\circ$ ) for nitro-BTC is shown in Fig. S21 (a). The nitro group is perpendicular to the benzene ring and is  $sp^2$  hybridized. The lone pair on the carboxylate oxygen atoms ( $O_{\text{ortho}}$ ), are planar with the benzene ring. For the ELF isosurface plotted at 0.87, no electron density is seen perpendicular to the nitro group. This can be attributed to the electron withdrawing effect of the more electronegative oxygen atoms and the double bond character of the N-O bond. The ELF for the minimum energy configuration ( $\theta = 123^\circ$  and  $\phi = 0^\circ$ ), shown in Fig. S21 (b), compares very well with the ideal tbo case and explains the nature of the contour plot and the energetic preference of the tbo topology.

**Table S8.** Comparison of DFT energies of the planar and perpendicular configuration of the functional group for the functionalized benzenes.

Linker	DFT Energy (kcal/mol)	Configuration	Energy Difference (kcal/mol)
<b>H-BTC</b>	-1752.7	-	-
<b>methyl</b>	-2136.2	-	-
<b>ethyl</b>	-2516.5	-	-
<b>methoxy</b>	-2278.2	planar	-4.1
	-2274.1	perpendicular	
<b>bromo</b>	-1704.2	-	-
<b>nitro</b>	-2108.8	planar	-5.4
	-2103.4	perpendicular	
<b>acetamide</b>	-2781.8	planar	-4.3
	-2777.5	perpendicular	
<b>amino</b>	-2032.2	planar	-9.8
	-2022.4	perpendicular	
<b>hydroxy</b>	-1907.4	planar	-4.5
	-1902.9	perpendicular	
<b>aldehyde</b>	-2106.2	planar	-8.9
	-2097.3	perpendicular	

### Analysis of functionalized benzenes

To gauge the effect of the ortho-carboxylate groups on the functional groups, it is useful to compare the geometry of the functional group in the BTC linker with corresponding functionalized benzene. The functionalized benzene molecules were energy minimized and the final energies for each structure are summarized in Table S8. For the planar functional groups (methoxy, nitro, acetamide, amino, hydroxy and aldehyde), we started with two configurations with the functional group being planar with the ring or perpendicular. Table S8 compares the



energy difference of the planar configuration with the perpendicular one and shows that for all these cases the planar configuration is always preferred. For the cases where the connecting atom is  $sp^2$  hybridized (C in aldehyde and N in nitro, acetamide and amino), the planar configuration allows for delocalization of the electrons over the benzene ring, which is not possible in a perpendicular configuration.

In the case of the functionalized BTC linker, the geometry of the functional group is affected by the presence of the -COO groups. In particular, due to the presence of the ortho-carboxylate groups in the actual BTC cluster, the planar configuration is only possible for the amino group due to its small size. This causes optimum geometry for the nitro and acetamide groups to be perpendicular to the ring.

#### Contour plots for other functional groups

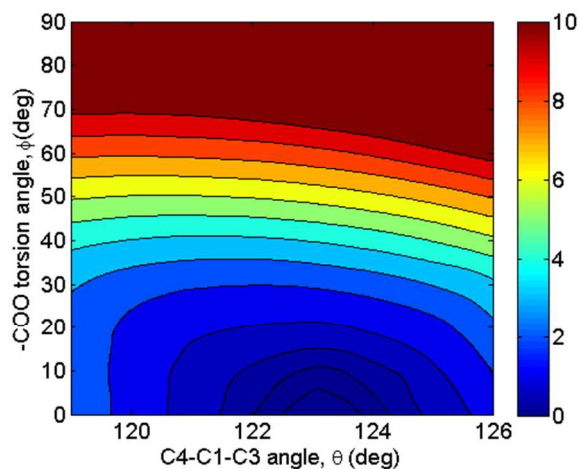


**Figure S23.** Contour plot of energy as a function of  $\phi$  and  $\theta$  for the hydroxy and functionalized BTC linker. Due to the small size of the -OH group, a planar configuration is preferred. Thus, even though the O atom is  $sp^3$  hybridized, the contour plot is similar to amino-BTC and the topology is preferred.

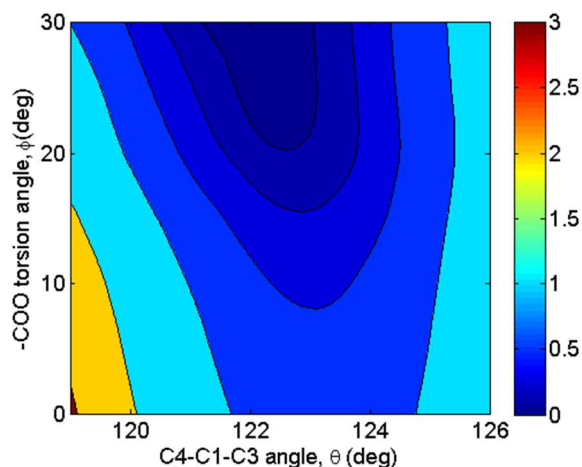


**Figure S24.** Contour plot of energy as a function of  $\phi$  and  $\theta$  for the fluoro functionalized BTC linker. The scenario is similar to bromo-BTC and the tbo topology is not preferred.

## References

- 1 Cai, Y., Zhang, Y., Huang, Y., Marder, S. R. & Walton, K. S. Impact of Alkyl-Functionalized BTC on Properties of Copper-Based Metal–Organic Frameworks. *Crystal Growth & Design* **12**, 3709-3713, doi:10.1021/cg300518k (2012).
- 2 Chui, S. S. A Chemically Functionalizable Nanoporous Material  $[\text{Cu}_3(\text{TMA})_2(\text{H}_2\text{O})_3]_n$ . *Science* **283**, 1148-1150, doi:10.1126/science.283.5405.1148 (1999).
- 3 Düren, T., Millange, F., Férey, G., Walton, K. S. & Snurr, R. Q. Calculating Geometric Surface Areas as a Characterization Tool for Metal–Organic Frameworks. *The Journal of Physical Chemistry C* **111**, 15350-15356, doi:10.1021/jp074723h (2007).